



Universiteit  
Leiden  
The Netherlands

## Stress, obesity and mood disorders: towards breaking a vicious cycle

Koorneef, L.L.

### Citation

Koorneef, L. L. (2021, October 6). *Stress, obesity and mood disorders: towards breaking a vicious cycle*. Retrieved from <https://hdl.handle.net/1887/3215051>

Version: Publisher's Version

License: [Licence agreement concerning inclusion of doctoral thesis in the Institutional Repository of the University of Leiden](#)

Downloaded from: <https://hdl.handle.net/1887/3215051>

**Note:** To cite this publication please use the final published version (if applicable).



# 5

## Selective glucocorticoid receptor modulation prevents and reverses non-alcoholic fatty liver disease in male mice

Lisa L. Koorneef\*  
José K. van den Heuvel\*  
Jan Kroon  
Mariëtte R. Boon  
Peter A.C. 't Hoen  
Kristina M. Hettne  
Nienke M. van de Velde  
Kelsey B. Kolenbrander  
Trea C.M. Streefland  
Isabel M. Mol  
Hetty C.M. Sips  
Szymon M. Kielbasa  
Hailiang Mei  
Joseph K. Belanoff  
Alberto M. Pereira  
Maaïke H. Oosterveer  
Hazel Hunt  
Patrick C.N. Rensen  
Onno C. Meijer

*\*Authors contributed equally*

*Endocrinology. 2018 Dec 1;159(12):3925-3936*

**ABSTRACT**

Medication for non-alcoholic fatty liver disease (NAFLD) is an unmet need. Glucocorticoid (GC) stress hormones drive fat metabolism in the liver, but both full blockade and full stimulation of GC signaling aggravate NAFLD pathology. We investigated the efficacy of selective glucocorticoid receptor (GR) modulator CORT118335, which recapitulates only a subset of GC actions, in reducing liver lipid accumulation in mice. Male C57BL/6J mice received low-fat diet, or high-fat diet mixed with vehicle or CORT118335. Livers were analyzed histologically and for genome-wide mRNA expression. Functionally, hepatic long-chain fatty acid (LCFA) composition was determined by gas chromatography. We determined very-low-density-lipoprotein (VLDL) production by treatment with a lipoprotein lipase inhibitor after which blood was collected to isolate radiolabeled VLDL particles and ApoB proteins. CORT118335 strongly prevented and reversed hepatic lipid accumulation. Liver transcriptome analysis showed increased expression of GR target genes involved in VLDL production. Accordingly, CORT118335 led to increased lipidation of VLDL particles, mimicking physiological GC action. Independent pathway analysis revealed that CORT118335 lacked induction of GC-responsive genes involved in cholesterol synthesis and LCFA uptake, which was indeed reflected in unaltered hepatic LCFA uptake *in vivo*. Our data thus reveal that the robust hepatic lipid lowering effect of CORT118335 is due to a unique combination of GR-dependent stimulation of lipid (VLDL) efflux from the liver, with a lack of stimulation of GR-dependent hepatic fatty acid uptake. Our findings firmly demonstrate the potential use of CORT118335 in the treatment of NAFLD and underscore the potential of selective GR modulation in metabolic disease.

## INTRODUCTION

Non-alcoholic fatty liver disease (NAFLD) is a prevalent condition (20%-30% of the general population) with rising incidence due to the obesity pandemic, and to date long-term treatment options are restricted to weight loss surgery [1, 2]. NAFLD can advance to non-alcoholic steatohepatitis and further progress toward hepatic fibrosis, cirrhosis and hepatocellular carcinoma [3]. NAFLD is caused primarily by an imbalance of hepatic energy influx and efflux. Because glucocorticoid (GC) hormones have a strong effect on hepatic energy homeostasis, modulation of GC signaling seems to be an interesting treatment option [4].

GCs (predominantly cortisol in humans and corticosterone in rodents) are secreted by the adrenal cortex during stress, to support recruitment of energy reserves for the organism, and follow a diurnal rhythm. These effects are mediated by the glucocorticoid receptor (GR), a member of the nuclear receptor superfamily [5]. Among the widespread effects of GCs are the regulation of metabolic pathways in the liver, including the stimulation of both the hepatic *influx* (uptake of free fatty acids and lipoproteins and via *de novo* lipogenesis) and *efflux* of lipids (via very-low-density-lipoprotein (VLDL) production) [6, 7]. Because GCs control distinct pathways that induce *and* prevent steatosis, both excessive GC exposure and GR antagonism can promote development of liver steatosis and fibrosis [8, 9].

Selective GR modulators combine GR agonism and antagonism that, upon binding to GRs, induce unique receptor conformations that allow interaction with only subsets of downstream signaling pathways. Therapeutic potential has long been recognized for inflammatory disease, but unequivocal *in vivo* data remain limited, in particular in clinical settings [10-12]. CORT118335 is a selective modulator that induces a profile of GR-coregulator interactions intermediate to full agonists and antagonists [13-15]. In the current study, we demonstrate that CORT118335 fully prevents and reverses hepatic lipid accumulation in high-fat diet (HFD)-fed mice, highlighting the promise of selective GR modulation in metabolic disease.

## MATERIALS AND METHODS

### Animal handling

The institutional ethics committee on animal care and experimentation at the Leiden University Medical Center (LUMC) approved all animal experiments that were conducted in Leiden (DEC13087 and DEC14245). Experiments were performed in 8-week old male C57Bl/6J mice (Charles River, France). Mice were individually housed in conventional cages with a 12:12 h light-dark cycle with *ad libitum* access to food and water. Through-

out metabolic experiments, body weight was determined twice a week and body composition was monitored weekly using EchoMRI<sup>tm</sup>. To investigate the metabolic effects of CORT118335, mice were randomized according to body weight to receive synthetic low-fat diet (LFD) or 10% fructose water with high-fat diet (HFD) (60% lard, Research Diets, USA) containing vehicle, CORT118335 (60 mg/kg/day), dexamethasone (1 mg/kg/day) or mifepristone (60 mg/kg/day). To evaluate the efficacy of CORT118335 in a more severe NAFLD model with noncontinuous drug administration, mice received a 16 week run-in HFD (45% lard, Research Diets, USA), after which they were randomized according to body weight to a 3-week oral gavage treatment with vehicle or CORT118335. Because peak drug levels are higher with oral administration, drug doses were decreased to 5 and 30 mg/kg/day. This study was carried out at RenaSci (Nottingham, United Kingdom). For RNA sequencing and determination of hepatic lipid composition, mice received an LFD, HFD supplemented with vehicle, CORT118335 (60 mg/kg/day) or corticosterone (10 mg/kg/d) for two days (n=4 per group). The rationale for the higher dose of CORT118335 was our hypothesis that part of its beneficial effects would depend on GR antagonism, requiring full receptor occupancy, whereas the dose of 10 mg/kg/day for corticosterone suffices for substantial agonist effects. For all experiments, mice were euthanized by cervical dislocation and perfused with ice-cold PBS after which tissues were collected for further analysis.

### **Indirect calorimetry**

At the start of the diet intervention, mice were transferred into fully automated metabolic cages for indirect calorimetry measurements (LabMaster System, TSE Systems, Germany). After 20 h of acclimatization, oxygen consumption ( $\dot{V}O_2$ ), carbon dioxide production ( $\dot{V}CO_2$ ) and caloric intake were measured for 5 consecutive days. Carbohydrate and fat oxidation rates, and total energy expenditure (EE) were calculated from  $\dot{V}O_2$  and  $\dot{V}CO_2$  as described previously [16].

### **Intravenous glucose tolerance test**

Mice were fasted for 6 h before the experiment. At t=0, blood was collected to measure basal plasma glucose, triglyceride and cholesterol levels. Next, a glucose bolus was injected (2 g/kg) and at t=5, t=15, t=30, t=60 and t=120 minutes tail blood was collected, and plasma glucose levels were measured (Instruchemie, Netherlands).

### **Corticosterone and ACTH measurements**

Basal plasma corticosterone and ACTH levels were measured in blood that was collected within 60 or 120 seconds after tail incision - *i.e.* before ACTH and corticosterone levels rise respectively - at AM (8:00) and PM (18:00). During the novelty stress test, at t=0 a blood sample was collected after which mice were placed into a cage without bedding.

After 10 minutes a blood sample was collected after which mice were placed back into their original home cage and additional stress-free blood samples were collected at t=30, t=60 and t=120. Plasma corticosterone levels were determined using  $^{125}\text{I}$  RIA kits (MP Biochemicals), with 25 ng/mL as the lowest detection limit and coefficients of variation of less than 20%. Plasma ACTH levels were determined using the Double Antibody hACTH  $^{125}\text{I}$  RIA kit (MP Biomedical), with 7 pg/mL as the lowest detection limit and coefficients of variation of less than 20%.

### **VLDL production measurement.**

Mice were fasted for 4 h and subsequently anaesthetized with 6.25 mg/kg acepromazine (Alfasan, the Netherlands), 6.25 mg/kg midazolam (Roche, the Netherlands) and 0.31 mg/kg fentanyl (Janssen-Cilag, the Netherlands). At t= -30 minutes, 20  $\mu\text{Ci}$  Tran $^{35}\text{S}$  label (S-35 Methionine; MP Biomedicals, USA) was injected into the tail vein. At t=0, the LPL inhibitor Triton WR 1339 (0.5 g/kg) (Tyloxapol; Sigma-Aldrich, Netherlands) was additionally intravenously injected, At t=0, 15, 30, 60 and 90 minutes blood was collected from the tail vein and at t= 120 mice were exsanguinated via the orbital sinus and euthanized with an overdose of anesthesia. VLDL was isolated from serum after density gradient ultracentrifugation at  $d < 1.006$  g/ml by aspiration [17]. ApoB proteins were next isolated by precipitation with isopropanol and examined for incorporated  $^{35}\text{S}$  activity.

### **Hepatic lipid determination with Cobas C111 analyzer**

To extract lipids, HPLC grade isopropanol (Fisher, USA) was added to liver samples (1mL/100 mg of tissue). To dissolve lipids, tissues were homogenized, revortexed and centrifuged to incubate at 70 °C for 25 minutes. Tubes were re-vortexed to remove undissolved matter and the supernatant was assayed for triglycerides and cholesterol using the Cobas C111 clinical analyzer (Roche, USA) and associated reagents. The concentration of liver lipids was expressed as the concentration in the original tissue by multiplying by 10 as the liver sample was extracted in 10 volumes of isopropanol.

### **Hepatic lipid determination with Bligh and Dyer**

Lipids were extracted from livers according to a modified protocol from Bligh and Dyer [18]. Liver samples were homogenized in ice-cold methanol and lipids were extracted into an organic phase (methanol : chloroform = 3:1). After centrifugation, the lower, organic phase was dried and suspended in 2% Triton X-100. Hepatic triglyceride (TG) and total cholesterol (TC) concentrations were measured using commercial enzymatic kits (Roche Diagnostics, Netherlands). Liver lipids were reported per milligram of protein, as determined using the BCA protein assay kit (Thermo Scientific, Rockford, USA).

### **Hepatic long-chain fatty acid determination**

Frozen liver tissue was homogenized in PBS and fatty acids were transmethylated to quantify fatty acid composition by gas chromatography using C17:0 as the internal standard [19].

### **Plasma lipid determination**

Blood was collected in paraxon-coated capillaries (Sigma-Aldrich, Netherlands) and triglyceride (TG), total cholesterol (TC), and phospholipid (PL) content was measured using commercially available enzymatic kits for TG, TC (Roche Diagnostics, Netherlands) and PL (Instruchemie, The Netherlands).

### **Lipoprotein profiles**

To determine the distribution of cholesterol and triglycerides over the various lipoproteins, pooled plasma samples (n= 8 per pool) were used for fast performance liquid chromatography (FPLC). Plasma was injected onto a Superose 6 column (Äkta System; Amersham Pharmacia Biotech, USA) and eluted at a constant flow rate (50 µl/min) with PBS (pH 7.4). In the collected fractions, TG and TC contents were measured as described previously.

### **RNA isolation, cDNA synthesis and real-time PCR**

Total RNA was isolated from frozen tissues utilizing Tripure RNA Isolation Reagent (Roche Applied Science, the Netherlands). mRNA was reverse-transcribed and cDNA was used for quantitative real-time PCR using IQ SYBR-Green supermix (MyIQ thermal cycler, Bio-RAD CFX96). Melt curve analysis was included to ensure a single PCR product and expression levels were normalized using the average expression of *Beta2-microglobulin* and *36b4* as housekeeping genes. Primer sequences are listed in **Sup. Table 1**.

### **Histological analysis**

Gonadal white adipose tissue (gWAT) and liver tissue were fixed in 4% paraformaldehyde for 24 h and stored in 70% ethanol until further processing. Tissues were dehydrated, embedded into paraffin and cut into 5 µm sections. Paraffin-waxed tissues were dewaxed and dehydrated before staining with Mayer's haematoxylin (Merck, the Netherlands) and eosin (Sigma-Aldrich, the Netherlands). Adipocyte size was quantified using ImageJ software (NIH, US [20]). For F4/80 staining, sections were permeabilized (with 0.1% Tween/PBS), endogenous peroxidases were quenched and antigens were retrieved with proteinase-K before incubation with a primary F4/80 antibody (1/600; Serotec, Oxford, UK, RRID:AB\_2098196, [https://antibodyregistry.org/AB\\_2098196](https://antibodyregistry.org/AB_2098196)) overnight. Sections were incubated with a goat anti-rat secondary antibody (ImmPRESS<sup>TM</sup>, Vector Laboratories, UK) for 30 minutes, stained with Nova Red (Vector Laboratories, UK) and counterstained

with Mayer's Haematoxylin. For oil red O staining, frozen hepatic tissue samples were cut in a degreased cryostat at  $-20^{\circ}\text{C}$  at  $10\ \mu\text{m}$ . Sections were fixed with formalin, rinsed with isopropanol, stained with filtered oil red O working solution ( $3\ \text{g/L}$ ), counterstained with Mayer's Haematoxylin and mounted with Kaiser's glycerine jelly.

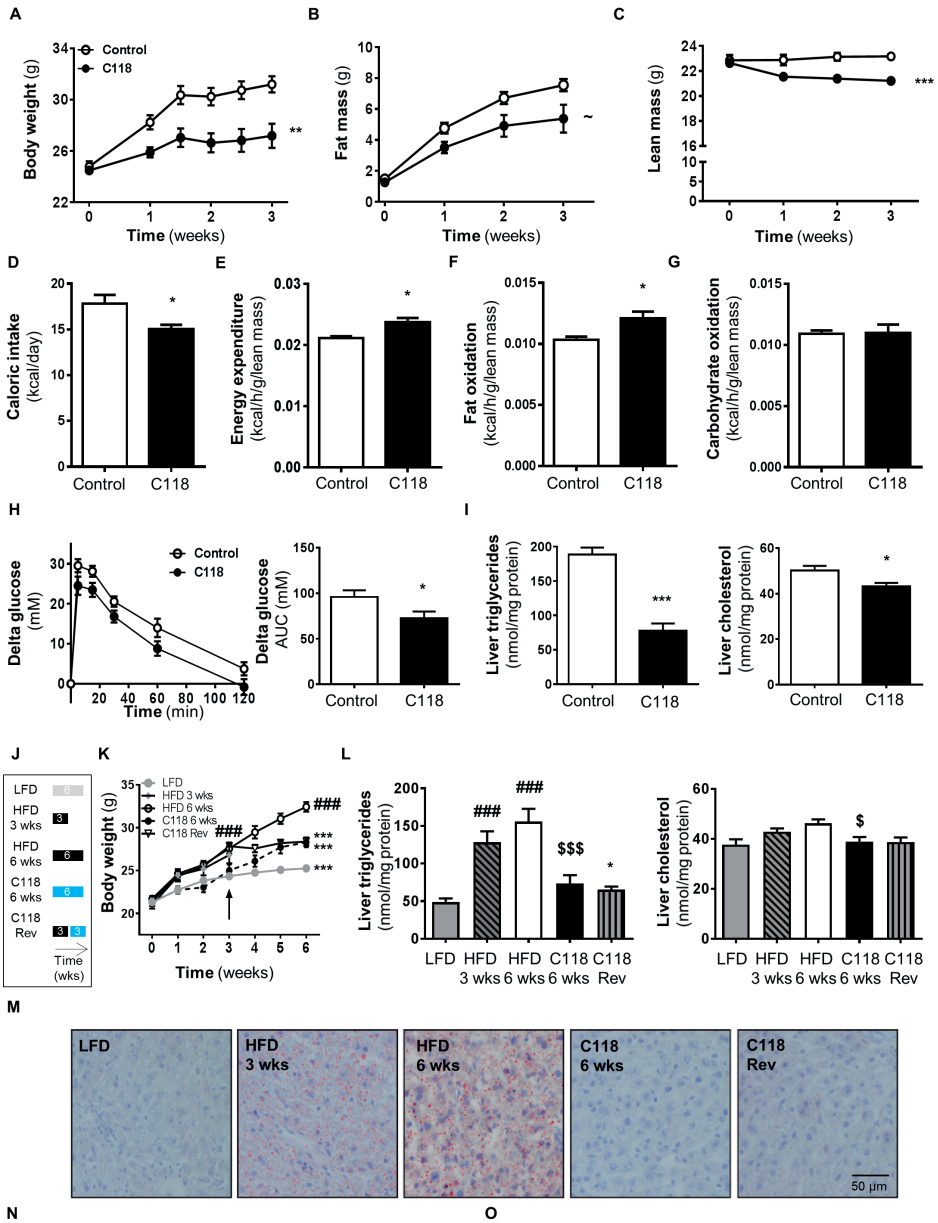
### RNA sequence analysis

Library construction and RNA sequencing were performed at BGI Tech Solutions CO., LTD (Hong kong, China). Briefly, isolated RNA was fragmented and first and second cDNA strands were synthesized. Adapters were ligated to A-tailed mRNA molecules with repaired ends, and cDNA fragments were enriched by PCR amplification and purified for 100-bp paired-end sequencing with the HiSeq 4000 System (HiSeq 3000/4000 SBS Kit, Illumina). All RNA sequence files were processed using the BIOPET Gentrapp pipeline version 0.6 developed at the LUMC ([http://biopet-docs.readthedocs.io/en/latest/releasenotes/release\\_notes\\_0.6.0/](http://biopet-docs.readthedocs.io/en/latest/releasenotes/release_notes_0.6.0/)). The pipeline includes the processes of quality control (with FastQC version 0.11.2), quality trimming (with Sickle version 1.33), adapter clipping (with Cutadapt version 1.9.1), RNA sequence alignment (with GSNAP version 2014-12-23, with mm10 as reference genome), gene annotation (on 11-09-2015 information was downloaded from UCSC), read and base quantification (with htseq-count version 0.6.1p1 with settings of "--stranded no") and low quality read trimming. After the BIOPET Gentrapp pipeline was run, a differential expression analysis was performed with the edgeR package using R software [21]. To correct for multiple testing, the Benjamini and Hochberg's False Discovery Rate (FDR) was put at 5%. Z- Scores data represent the distribution of normalized gene counts across all conditions for genes that showed significant differences between any of the groups. For pathway and mind map analyses, the Euretoto-Knowledge Platform was used (<http://Euretoto.com/>). Euretoto allows semantic searches for biologically interesting connections between genes, proteins, metabolites and drugs based on an underlying database of 176 integrated data sources (January 2017) [<http://www.euretoto.com/files/EKPSources2017.pdf>]. Data from these databases were obtained in June 2017. Pathway analysis was performed by using the Fisher exact test for gene set enrichment.

### Statistical analysis

All data are expressed as mean  $\pm$  SEM. All p-values were two-tailed and  $p < 0.05$  was considered statistically significant. Data concerning one factor and two groups were analyzed with an independent sample T-test. When one factor and more than two groups were investigated, a one-way ANOVA with Fisher's post-hoc test was performed. When the data concerned were both a factor and a time component, a mixed model analysis was performed in which time was modelled as factor with less than four time points and as covariate with four or more time points.





Treatment	Triglycerides (μmoles/g)		
	mean	SEM	P-value
Vehicle	120,7	26,1	
CORT118335 5 mg/kg	70,8	11,1	0,0876
CORT118335 30 mg/kg	47,8	11,9	0,0088**

Treatment	Cholesterol (mg/g)		
	mean	SEM	P-value
Vehicle	1,5	0,2	
CORT118335 5 mg/kg	1,8	0,1	0,8974
CORT118335 30 mg/kg	1,4	0,1	0,4152

← **Figure 1: CORT118335 prevents and reverses hepatic lipid accumulation.** In a preventive setting, mice received 10% fructose water and a high-fat diet (HFD) containing vehicle or CORT118335 (C118) for three weeks (n=8 per group). A-C) C118 reduced body weight, fat mass and lean mass. D-G) C118 additionally reduced caloric intake, energy expenditure and fat oxidation but not carbohydrate oxidation in week 1. H) C118 increased intravenous glucose tolerance in week 2; glucose levels shown are corrected for baseline. I) C118 strongly reduced hepatic triglycerides and cholesterol in week 2. J) In a reversal setting, mice received low-fat diet (LFD), 10% fructose water and a HFD supplemented with vehicle or C118, or HFD for three weeks followed by HFD supplemented with C118 for three weeks (Reversal or Rev, n=8 per group). K-L) C118 reduced body weight, and fully normalized hepatic triglycerides and cholesterol. M) Representative images of hepatic lipid staining using oil red O. In a more severe NAFLD model, mice received HFD for 16 weeks after which treatment with vehicle or C118 (5 and 30 mg/kg/day) was started. N-O) C118 dose-dependently reduced hepatic triglycerides but not cholesterol. ~ = p<0.1 vs HFD 3 wks; \* = p<0.05, \*\* = p<0.01, \*\*\* = p<0.001 vs HFD 3 wks; \$ = p<0.05, \$\$\$ p<0.001 vs HFD 6 wks; ### = p<0.001 vs LFD.

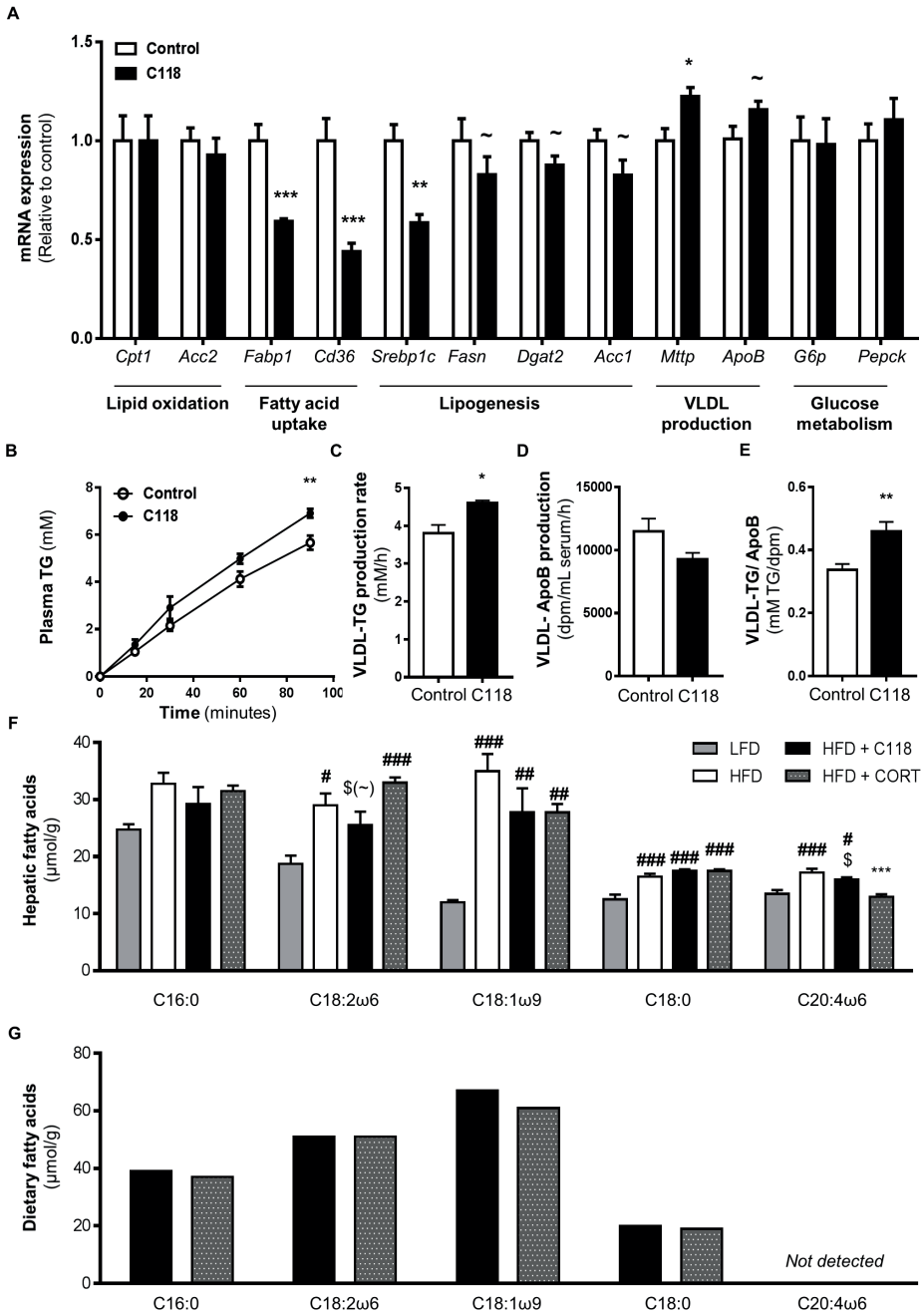
## RESULTS

### CORT118335 prevents obesity and hepatic accumulation of triglycerides and cholesterol

To evaluate the effect of CORT118335 on obesity and related metabolic parameters, male C57BL/6J mice received HFD supplemented with either vehicle (control) or CORT118335 for three weeks. CORT118335 significantly attenuated body weight gain (**Fig. 1A**), caused by a reduction of both fat mass (**Fig. 1B, Sup. Fig. 1A-C**) and lean mass (**Fig. 1C**). Indirect calorimetry measurements in the first week of treatment showed that CORT118335 treatment reduced caloric intake while increasing energy expenditure and fat oxidation, but not carbohydrate oxidation (**Fig. 1D-G**). Oral glucose tolerance was improved upon CORT118335 treatment (**Fig. 1H**). In addition to the overall attenuation of HFD-induced adverse metabolic consequences, CORT118335 elicited a large reduction of hepatic triglycerides (-59%, p<0.001) and cholesterol (-14%, p=0.02), which was confirmed by oil red O staining (**Fig. 1I, Sup. Fig. 1D**). Liver weight was reduced after CORT118335 treatment (**Sup. Fig. 1E**) and so was hepatic inflammation as determined by F4/80 immunostaining (**Sup. Fig. 1F**).

### CORT118335 reverses hepatic accumulation of triglycerides and cholesterol

In view of the substantial change in liver lipid content after CORT118335 treatment, we next evaluated the capacity of CORT118335 to *reverse* the accumulation of hepatic lipids. Mice received either low-fat diet (LFD), HFD for three or six weeks, HFD with CORT118335 for six weeks ('prevention') or HFD for three weeks followed by HFD with CORT118335 ('reversal', **Fig. 1J**). CORT118335 treatment attenuated HFD-induced body weight gain, in both the prevention and the reversal settings (**Fig. 1K**). CORT118335 effectively normalized hepatic triglycerides and cholesterol levels to those observed after an LFD in both CORT118335 prevention and reversal treatment groups (**Fig. 1L-M**). Plasma cholesterol levels were increased in CORT118335-treated mice, which was



← **Figure 2: CORT118335 increases hepatic VLDL-triglyceride production and decreases long-chain fatty acid uptake.** A) In a preventive setting, mice received 10% fructose water with high-fat diet (HFD) containing vehicle or CORT118335 (C118). C118 selectively affected expression of genes related to hepatic lipid but not to glucose metabolism after three weeks (n=8 per group). B-C) VLDL production measurements after two days of C118 or vehicle treatment in mice that received HFD for 2.5 weeks (n=8 per group) showed that C118 increased plasma triglyceride accumulation after inhibition of tissue lipoprotein lipase, i.e. VLDL-TG production rate. D-E) The amount of produced VLDL particles was not different as measured with  $\text{Tran}^{35}\text{S}$  labelling of apolipoproteins, CORT118335 rather increased the amount of TG per apoB. F) Long-chain fatty acid composition indicated C118 reduced fatty acid uptake as compared to corticosterone treatment (C18:2w6), but did not alter *de novo* lipogenesis (C20:4w6). Mice received low-fat diet (LFD), high-fat diet (HFD) supplemented with vehicle, C118 or corticosterone for two days (n=4 per group) and in G) respective diets. \* =  $p < 0.05$ , \*\* =  $p < 0.01$ , \*\*\* =  $p < 0.001$  vs HFD; # =  $p < 0.05$ , ## =  $p < 0.01$ , ### =  $p < 0.001$  vs LFD; \$(-) =  $p < 0.01$ , \$ =  $p < 0.05$  vs corticosterone.

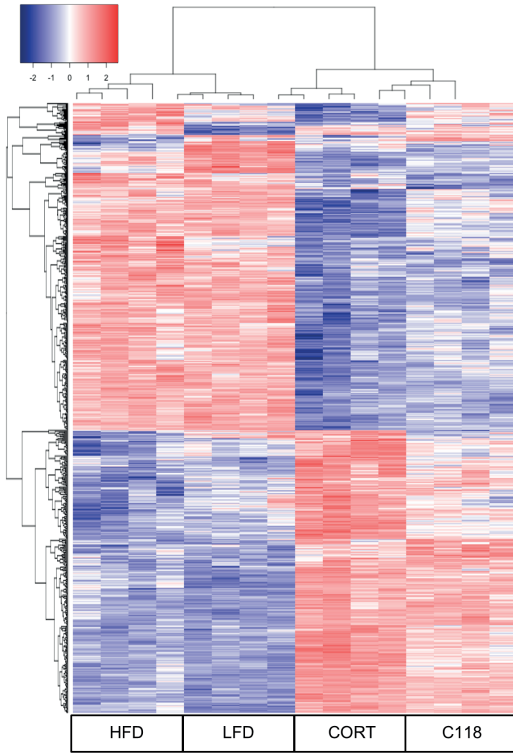
mostly due to an increased high-density-lipoprotein fraction (**Sup. Fig. 2A-B**). To investigate whether CORT118335 reversed liver steatosis in a more severe NAFLD model with noncontinuous drug administration, mice received 45% HFD for 16 weeks after which they received CORT118335 treatment via oral gavage for three weeks. CORT118335 strongly and dose-dependently reduced liver triglycerides (-41% and -60%,  $p=0.09$  and  $p=0.009$  respectively, **Fig. 1N**) but not liver cholesterol (**Fig. 1O**).

To confirm that selective GR modulation is essential to the improved liver phenotype, the full GR agonist dexamethasone and the full GR antagonist mifepristone were investigated. Both dexamethasone and mifepristone did not improve, and even aggravated, hepatic triglyceride accumulation (**Sup. Fig. 3A-C**), despite the fact that mifepristone significantly reduced food intake in this experiment (**Sup. Fig. 3D**). This strongly supports the notion that the effects of CORT118335 on hepatic lipid content can be attributed to selective GR modulation.

### CORT118335 stimulates hepatic VLDL-triglyceride production

Because liver steatosis develops as result of an imbalance in hepatic lipid metabolism pathways, expression of genes within these pathways was investigated in vehicle- and CORT118335-treated mice after three weeks of treatment. CORT118335 upregulated the expression of genes involved in VLDL production and secretion (i.e. *ApoB*, *Mttp*) but not the expression of genes involved in beta-oxidation (i.e., *Cpt1a*, *Acc2*) (**Fig. 2A**). Genes involved in fatty acid uptake (i.e. *Fabp1*, *Cd36*) were downregulated (**Fig. 2A**) as were genes involved in *de novo* lipogenesis (*Srebp1c*, *Fasn*, *Dgat2*, *Acc1*, **Fig. 2A**). Next, we investigated whether the CORT118335-induced upregulation of *Mttp* and *ApoB* expression was associated with increased VLDL production by assessing plasma triglyceride accumulation after inhibition of tissue lipoprotein lipase while labeling apolipoproteins with  $\text{Tran}^{35}\text{S}$ . In line with the transcriptional data, CORT118335 treatment led to increased plasma triglyceride accumulation over time (**Fig. 2B-C**). Increased hepatic VLDL output involved enhanced lipidation of VLDL particles rather than increased VLDL particle production, as the amount of triglycerides per apoB, but not plasma apoB, was significantly elevated in CORT118335-treated mice (**Fig. 2D-E**). Because the MTP

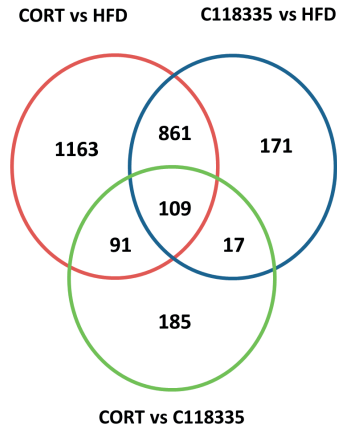
A



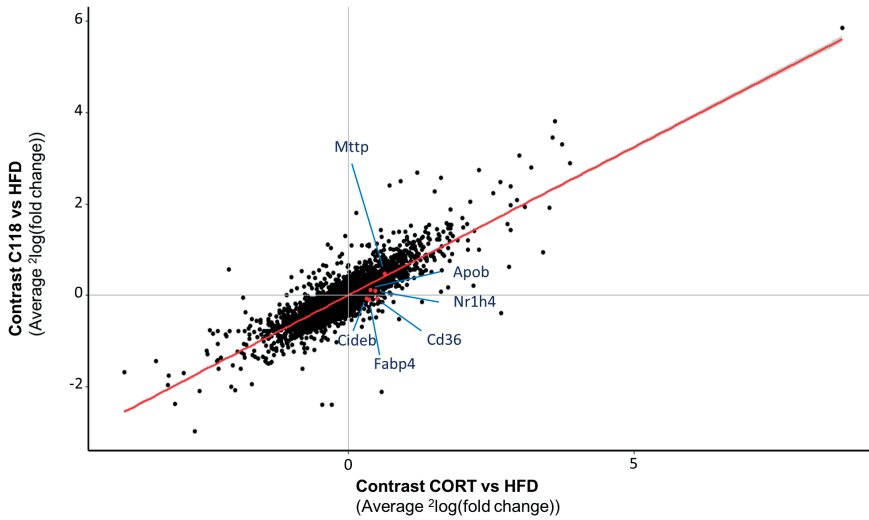
B

Comparisons	#DE	# Up	# Down
HFD vs LFD	402	189	213
CORT vs HFD	2224	1085	1139
C118 vs HFD	1158	548	610
CORT vs C118	349	171	178

C



D



← **Figure 3: CORT118335 is a selective GR modulator with predominantly partial agonistic properties on hepatic gene expression.** RNA sequence analysis was performed on livers of mice that received low-fat diet (LFD), 10% fructose water and a high-fat diet (HFD) supplemented with vehicle, CORT118335 (C118) or corticosterone (CORT) for two days (n=4 per group). A) Heatmap of clustered Z-scores based on the fit to the distribution of normalized gene counts across all conditions for genes that showed significant ( $P < 0.00001$ ) differences between any of the groups B) The number of differentially expressed genes in four different comparisons, 1) HFD vs LFD diet, 2) CORT vs HFD, 3) C118 vs HFD and 4) CORT vs C118, reveal that C118 regulates half as many genes as CORT. C) Venn diagram of overlap of up- and downregulated genes between different comparisons. D) The slope of the average log fold change induction by C118 versus CORT indicates an intrinsic efficacy of 0.65 for most genes, but one that is substantially lower for some genes.

protein is responsible for the intracellular lipidation of apoB to generate VLDL [22], the upregulation of *Mttp* rather than *ApoB* mRNA appears to be predominantly involved in the biological effect of CORT118335 on VLDL-triglyceride production.

### CORT118335 inhibits fatty acid uptake by the liver

We next investigated whether the reduction of fatty acid transporter gene transcription after CORT118335 treatment (**Fig. 2A**) was accompanied by functional alterations and how these effects were related to receptor (ant)agonism. To this end, long-chain fatty acids (LCFA) were quantified in the livers of mice after 2 days of treatment with an LFD, HFD or HFD supplemented with CORT118335 or with corticosterone (**Fig. 2F**). The essential fatty acid C18:2 $\omega$ 6 is a measure for hepatic LCFA uptake as it is exclusively diet-derived and cannot be synthesized *de novo*. CORT118335 tended to reduce hepatic C18:2 $\omega$ 6 content as compared with content in corticosterone-treated animals, suggesting that CORT118335 decreased hepatic fatty acid uptake. After six weeks of CORT118335 treatment, these effects were more pronounced as hepatic C18:2 $\omega$ 6 LCFA levels were fully normalized to LFD levels (**Sup. Fig. 4A**). C20:4 $\omega$ 6 LCFA was absent from the diet (**Fig. 2G**) and therefore reflects elongation of lipids after uptake and *de novo* lipogenesis. Both corticosterone and CORT118335 significantly reduced C20:4 $\omega$ 6 content, although the effect of corticosterone was larger (**Fig. 2F**).

### CORT118335 combines partial GR agonistic and antagonistic properties

To identify the early beneficial transcriptional effects of CORT118335, we performed whole transcriptome analysis on livers of mice after two days of treatment with an LFD, HFD, or HFD supplemented with CORT118335 or with corticosterone. The overall gene expression profiles of corticosterone- and CORT118335-treated mice were comparable, as well as those of HFD and LFD groups (**Fig. 3A**). In a HFD condition, corticosterone regulated roughly twice as many genes as CORT118335 (**Fig. 3B**). Most CORT118335-regulated genes were also regulated by corticosterone (**Fig. 3C**). Comparison of gene induction by corticosterone and CORT118335 indicated that, despite the higher dosage of CORT118335 and similar  $K_d$ , the latter acted as a partial GR agonist with an intrinsic efficacy of 0.65, as calculated from the slope of the regression line (**Fig. 3D**). Examples

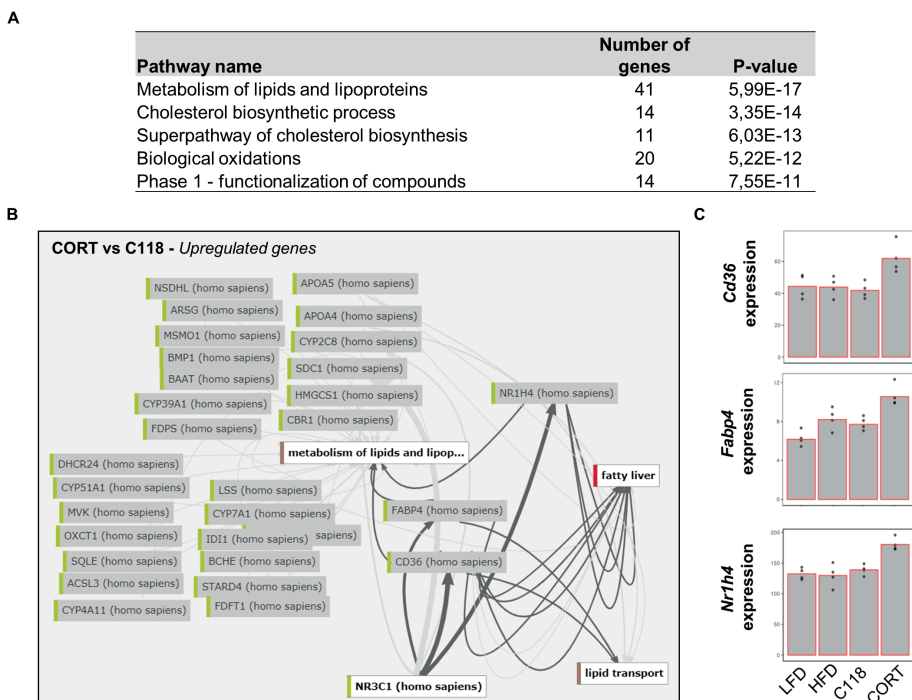


**Figure 4: Corticosterone, but not CORT118335, upregulates expression of genes involved in hepatic fatty acid uptake.** RNA sequence analysis was performed on livers of mice that received low-fat diet (LFD), 10% fructose water and a high-fat diet (HFD) supplemented with vehicle, CORT118335 (C118) or corticosterone (CORT) for two days (n=4 per group). A) Pathway analysis on differentially expressed genes in the CORT vs C118 comparison indicated that corticosterone regulated lipid metabolism-related genes stronger than C118 in a HFD context. B) Relationships between upregulated genes within the 'Metabolism of lipids and lipoprotein' pathway and 'fatty liver', 'Nr3c1' (glucocorticoid receptor gene), and 'lipid transport'. C) Hepatic expression of candidate genes.

of partial agonistic actions of CORT118335 include the upregulation of classical GR target genes *Per1* and *Fkbp5*, and recently identified hepatic GR target genes *As3mt* and *Herpud1* [23] after CORT118335 treatment (Sup. Fig. 5A). Other genes were strongly regulated by corticosterone but not, or to a much lesser extent by CORT118335 (Fig. 3D). Expression of GR target genes *Mt1*, *Mt2*, *Abi1* and *Comt* [23] clearly demonstrated lack of agonism of the compound (Sup. Fig. 5A). Partial agonism of CORT118335 on the GR was also evident from effects on *in vivo* Hypothalamus-Pituitary-Adrenal-axis (HPA-) dynamics, as the compound suppressed both basal and stress-induced endogenous corticosterone and ACTH plasma levels and reduced tissue weights of GC-sensitive thymus, adrenals and spleen (Sup. Fig. 5B-D).

## Corticosterone and CORT118335 differentially regulate lipid transport, cholesterol biosynthesis and cytokine signaling pathways

As the beneficial effects of CORT118335 can most likely be attributed to a combination of both GR agonism (e.g. VLDL production) and antagonism (e.g. fatty acid transport), we performed pathway analyses on *shared* and *differentially* regulated genes by corticosterone and CORT118335. *Shared* upregulated genes (Sup. Fig. 6A) were enriched for lipid, lipoprotein, glucose and glycogen metabolism pathways (Sup. Fig. 7A). Further subdivision of the ‘lipid metabolism’ pathway showed that both corticosterone and CORT118335 upregulated gene expression for *de novo* lipogenesis and beta oxidation (Sup. Fig. 6B). As expected, genes involved in VLDL production pathway, *Mttp* and *Apob*, were upregulated after both treatments (Sup. Fig. 6C). *Differentially* expressed genes between corticosterone and CORT118335 (n=349, Fig. 3B) showed significant enrichment of the ‘Metabolism of Lipids and Lipoproteins’ pathway’ (Fig. 4A). The genes selectively upregulated by corticosterone but not by CORT118335 were also enriched for lipid metabolism pathways (Sup. Fig. 7B) and some genes in this pathway were likely directly regulated by the GR (*Fabp4* [24], *Cd36* [25-28] and *Nr1h4* [25, 26, 28-30]) (Fig. 4B). Several selectively corticosterone-upregulated genes are associated with liver steatosis (*Cd36* [31-35], *Nr1h4* [35-37] and *Fabp4* [38, 39]) (Fig. 4B-C), and lipid transport (*Cd36* [40] and *Fabp4* [41]). Of note, corticosterone, but not CORT118335, also upregulated genes of cholesterol biosynthesis pathways (Sup. Fig. 7B). Among these differently regulated genes was *Hmgcs1*, which encodes for one of the rate-limiting enzymes in cholesterol biosynthesis and is a direct target gene of the GR (Sup. Fig. 7C) [25, 26, 28, 29]. To investigate the effects of CORT118335 on GR-mediated transrepression mechanisms, pathway analysis was performed on genes that were specifically downregulated by corticosterone but not by CORT118335. This revealed that corticosterone but not CORT118335 downregulated ‘Cytokine Signaling in Immune System’ and ‘Jak-Stat signaling’ pathways (Sup. Fig. 7D).

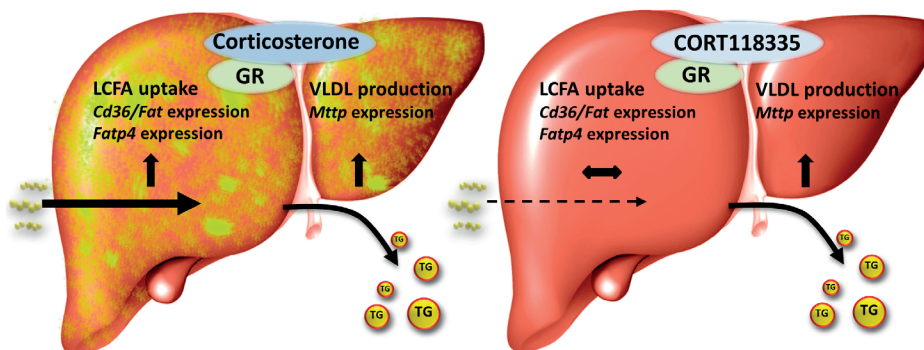


Figure 5: Graphical abstract



## DISCUSSION

Our data firmly demonstrated that CORT118335 prevents and reverses liver steatosis in mice. To support daily activity and adaptation to stress, endogenous GC are known to increase the flux of hepatic lipids by increasing VLDL production as well as lipid uptake [42, 43], effects that are predominantly GR-mediated (**Fig. 5**) [18]. CORT118335 selectively recapitulates the lipid outflow component via GR agonism, while lacking lipid uptake promoting activities, altogether confirming its selective GR modulatory profile (**Fig. 5**) [13]. Our transcriptome analysis, early during intervention, showed predominant partial GR agonism in the liver, with some notable exceptions that are likely - and fortuitously - linked to prevention of hepatic lipid accumulation. The major factors involved in reduced hepatic lipid accumulation upon CORT118335 treatment are increased VLDL-triglyceride production, reduced LCFA uptake and potentially also increased whole-body fatty acid oxidation, as increased fatty acid oxidation in extra-hepatic tissues may reduce lipid flux toward the liver. In addition, reduced food intake, adiposity and *de novo* lipogenesis may contribute to the steatosis-reducing activities of CORT118335. The fact that mifepristone led to a comparable reduction in food intake in most experiments excludes this factor as the sole responsible mechanism. In this respect, pair feeding experiments can be of interest, but were not performed because food restriction is intrinsically stressful and would have strongly complicated our experimental results. In addition to its strong beneficial effects on the liver, CORT118335 treatment also improved overall metabolic health, which is exemplified by a reduction in body weight and improved glucose tolerance, reflecting increased insulin sensitivity. These effects are not unique to CORT118335, as other selective GR modulators such as CORT108297 and the GR antagonist mifepristone were shown to have similar metabolic activities [44, 45]. The robust effect of CORT118335 on liver lipids is distinctive from that of other GR ligands. Nevertheless, metabolic effects of CORT118335 may be a consequence of reduced hepatic lipid content, thereby improving insulin sensitivity and reducing inflammation [46]. Because transcriptome analysis showed that CORT118335 was less capable than corticosterone in transrepressing inflammatory pathways, it is unlikely that CORT118335 is a strong anti-inflammatory drug via classic GR-mediated transrepression [47]. The effects of CORT118335 on muscle (and bone) catabolism, as apparent from lean mass data, are most likely driven by (partial) GR agonistic actions and will be the focus of further investigation.

Although extrahepatic mechanisms may contribute to the effects of CORT118335, several facts argue for a strong direct effect on hepatocytes. Measurements of VLDL-triglyceride production, hepatic LCFA composition and the CORT118335-associated transcriptome were obtained very early after initiation of treatment, even before any substantial (diet-induced) differences in total liver lipid content had developed. In ad-

dition, the compound provokes a number of effects that have been found by the specific targeting of liver GR and very short term transcriptional changes [23]. The substantial body of data on liver lipids based on targeted GR manipulation also argues against a dominant role of the mineralocorticoid receptor at which CORT118335 acts as a lower affinity antagonist [14]. Thus, some liver-specific effects are exclusive for CORT118335 and do reduce NAFLD development.

Although full GR agonism stimulates lipid flux and full GR antagonism lowers lipid flux through the liver, neither leads to hepatic lipid depletion. Our transcriptome analysis supports the concept that the unique combination of partial agonism and antagonism at the GR is responsible for the beneficial liver activities of CORT118335. Corticosterone but not CORT118335 upregulated gene expression of two out of six known fatty acid transport proteins that are related to liver influx: *Cd36/Fat* and *Fatp4*. The involvement of CD36/FAT in liver steatosis has been shown as hepatocyte specific CD36/FAT knock-out mice were protected against HFD-induced hepatic lipid accumulation [34].

In addition to reducing hepatic TGs, CORT118335 had cholesterol-lowering activity. This effect seems to be the result of enhanced cholesterol efflux (VLDL-production) and, as suggested from our transcriptomics data, a lack of effect on cholesterol biosynthesis pathways (e.g. *Hmgcs1*). Reducing hepatic cholesterol levels, with for example HMG-coA inhibitors (statins), was shown to improve NAFLD and non-alcoholic steatohepatitis and was recently even suggested as a novel therapeutic strategy [48, 49].

Selective GR modulation or ‘dissociated signaling’ has been pursued as inflammatory disease treatment for decades [50]. Our data establish that it is feasible to use selective GR modulation to target GR-dependent diseases, by interfering with metabolic fluxes - not only in prevention, but also in a reversal setting. Further mechanistic studies on selective receptor modulators will help with understanding and predicting which GR transcriptional coregulators and signaling pathways are involved in pathogenic processes. In itself, CORT118335 forms an interesting lead for future clinical development.

## ACKNOWLEDGMENTS

We gratefully thank Sander van der Zeeuw for valuable assistance with bioinformatic analysis of the RNA sequence data. We also thank our colleagues at RenaSci (Nottingham) for conducting mouse experiments that were of great value to the manuscript.

## REFERENCES

1. Blachier, M., et al., *The burden of liver disease in Europe: a review of available epidemiological data*. J Hepatol, 2013. **58**(3): p. 593-608.
2. Rinella, M.E. and A.J. Sanyal, *Management of NAFLD: a stage-based approach*. Nat Rev Gastroenterol Hepatol, 2016. **13**(4): p. 196-205.
3. Vernon, G., A. Baranova, and Z.M. Younossi, *Systematic review: the epidemiology and natural history of non-alcoholic fatty liver disease and non-alcoholic steatohepatitis in adults*. Aliment Pharmacol Ther, 2011. **34**(3): p. 274-85.
4. Woods, C.P., J.M. Hazlehurst, and J.W. Tomlinson, *Glucocorticoids and non-alcoholic fatty liver disease*. J Steroid Biochem Mol Biol, 2015. **154**: p. 94-103.
5. Hollenberg, S.M., et al., *Primary structure and expression of a functional human glucocorticoid receptor cDNA*. Nature, 1985. **318**(6047): p. 635-41.
6. Yu, C.Y., et al., *Genome-wide analysis of glucocorticoid receptor binding regions in adipocytes reveal gene network involved in triglyceride homeostasis*. PLoS One, 2010. **5**(12): p. e15188.
7. Vegiopoulos, A. and S. Herzig, *Glucocorticoids, metabolism and metabolic diseases*. Mol Cell Endocrinol, 2007. **275**(1-2): p. 43-61.
8. D'Souza A, M., et al., *Consumption of a high-fat diet rapidly exacerbates the development of fatty liver disease that occurs with chronically elevated glucocorticoids*. Am J Physiol Gastrointest Liver Physiol, 2012. **302**(8): p. G850-63.
9. Warriar, M., et al., *Susceptibility to diet-induced hepatic steatosis and glucocorticoid resistance in FK506-binding protein 52-deficient mice*. Endocrinology, 2010. **151**(7): p. 3225-36.
10. Asagami, T., et al., *Selective Glucocorticoid Receptor (GR-II) Antagonist Reduces Body Weight Gain in Mice*. J Nutr Metab, 2011. **2011**: p. 235389.
11. Thiele, S., et al., *Selective glucocorticoid receptor modulation maintains bone mineral density in mice*. J Bone Miner Res, 2012. **27**(11): p. 2242-50.
12. Brandish, P.E., et al., *The preclinical efficacy, selectivity and pharmacologic profile of MK-5932, an insulin-sparing selective glucocorticoid receptor modulator*. Eur J Pharmacol, 2014. **724**: p. 102-11.
13. Atucha, E., et al., *A Mixed Glucocorticoid/Mineralocorticoid Selective Modulator With Dominant Antagonism in the Male Rat Brain*. Endocrinology, 2015. **156**(11): p. 4105-14.
14. Hunt, H.J., et al., *Discovery of a novel non-steroidal GR antagonist with in vivo efficacy in the olanzapine-induced weight gain model in the rat*. Bioorg Med Chem Lett, 2012. **22**(24): p. 7376-80.
15. Zalachoras, I., et al., *Differential targeting of brain stress circuits with a selective glucocorticoid receptor modulator*. Proc Natl Acad Sci U S A, 2013. **110**(19): p. 7910-5.
16. Van Klinken, J.B., et al., *Estimation of activity related energy expenditure and resting metabolic rate in freely moving mice from indirect calorimetry data*. PLoS One, 2012. **7**(5): p. e36162.
17. Redgrave, T.G., D.C. Roberts, and C.E. West, *Separation of plasma lipoproteins by density-gradient ultracentrifugation*. Anal Biochem, 1975. **65**(1-2): p. 42-9.
18. Bligh, E.G. and W.J. Dyer, *A rapid method of total lipid extraction and purification*. Can J Biochem Physiol, 1959. **37**(8): p. 911-7.
19. Muskiet, F.A., et al., *Capillary gas chromatographic profiling of total long-chain fatty acids and cholesterol in biological materials*. J Chromatogr, 1983. **278**(2): p. 231-44.

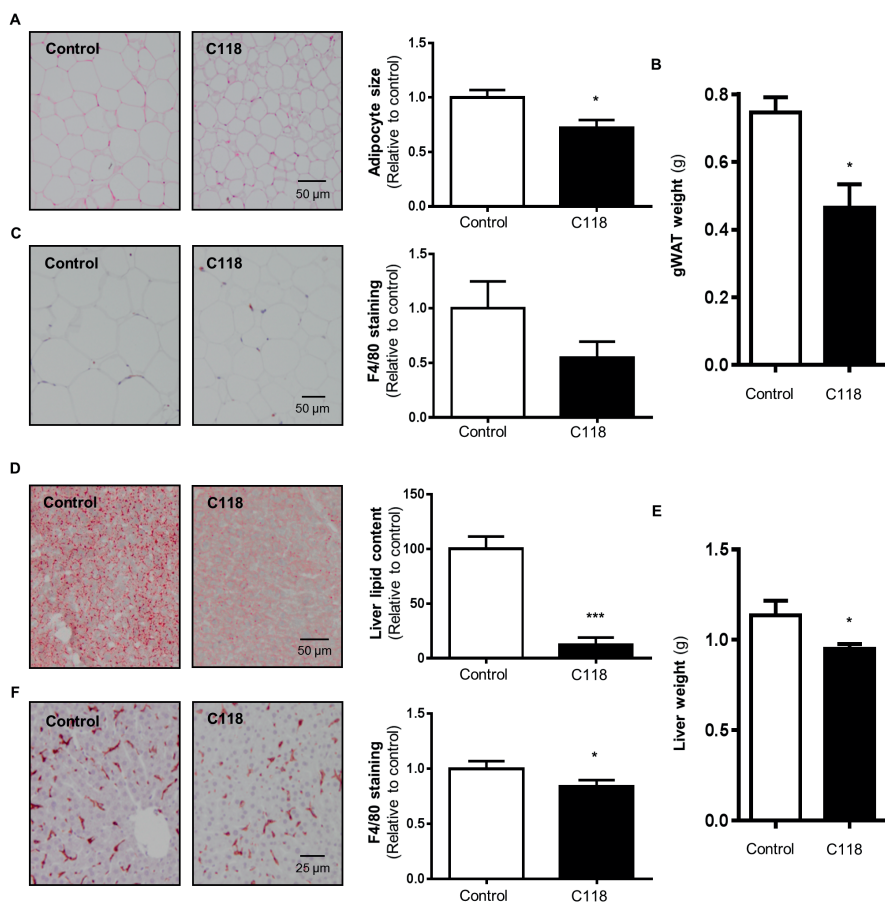
20. Schneider, C.A., W.S. Rasband, and K.W. Eliceiri, *NIH Image to ImageJ: 25 years of image analysis*. Nat Methods, 2012. **9**(7): p. 671-5.
21. McCarthy, D.J., Y. Chen, and G.K. Smyth, *Differential expression analysis of multifactor RNA-Seq experiments with respect to biological variation*. Nucleic Acids Res, 2012. **40**(10): p. 4288-97.
22. Shelness, G.S. and J.A. Sellers, *Very-low-density lipoprotein assembly and secretion*. Curr Opin Lipidol, 2001. **12**(2): p. 151-7.
23. Phuc Le, P., et al., *Glucocorticoid receptor-dependent gene regulatory networks*. PLoS Genet, 2005. **1**(2): p. e16.
24. Davis, A.P., et al., *The Comparative Toxicogenomics Database: update 2017*. Nucleic Acids Res, 2017. **45**(D1): p. D972-D978.
25. Cerami, E.G., et al., *Pathway Commons, a web resource for biological pathway data*. Nucleic Acids Res, 2011. **39**(Database issue): p. D685-90.
26. Wingender, E., *The TRANSFAC project as an example of framework technology that supports the analysis of genomic regulation*. Brief Bioinform, 2008. **9**(4): p. 326-32.
27. Orchard, S., et al., *The MIntAct project--IntAct as a common curation platform for 11 molecular interaction databases*. Nucleic Acids Res, 2014. **42**(Database issue): p. D358-63.
28. Chatr-Aryamontri, A., et al., *The BioGRID interaction database: 2017 update*. Nucleic Acids Res, 2017. **45**(D1): p. D369-D379.
29. Fabregat, A., et al., *The Reactome pathway Knowledgebase*. Nucleic Acids Res, 2016. **44**(D1): p. D481-7.
30. Milacic, M., et al., *Annotating cancer variants and anti-cancer therapeutics in reactome*. Cancers (Basel), 2012. **4**(4): p. 1180-211.
31. Declercq, J., et al., *Metabolic and Behavioural Phenotypes in Nestin-Cre Mice Are Caused by Hypothalamic Expression of Human Growth Hormone*. PLoS One, 2015. **10**(8): p. e0135502.
32. Yao, L., et al., *Hyperhomocysteinemia activates the aryl hydrocarbon receptor/CD36 pathway to promote hepatic steatosis in mice*. Hepatology, 2016. **64**(1): p. 92-105.
33. Zhou, J., et al., *Hepatic fatty acid transporter Cd36 is a common target of LXR, PXR, and PPARgamma in promoting steatosis*. Gastroenterology, 2008. **134**(2): p. 556-67.
34. Wilson, C.G., et al., *Hepatocyte-Specific Disruption of CD36 Attenuates Fatty Liver and Improves Insulin Sensitivity in HFD-Fed Mice*. Endocrinology, 2016. **157**(2): p. 570-85.
35. Pinero, J., et al., *DisGeNET: a comprehensive platform integrating information on human disease-associated genes and variants*. Nucleic Acids Res, 2017. **45**(D1): p. D833-D839.
36. Cote, I., et al., *An atherogenic diet decreases liver FXR gene expression and causes severe hepatic steatosis and hepatic cholesterol accumulation: effect of endurance training*. Eur J Nutr, 2013. **52**(5): p. 1523-32.
37. Martin, I.V., et al., *Bile acid retention and activation of endogenous hepatic farnesoid-X-receptor in the pathogenesis of fatty liver disease in ob/ob-mice*. Biol Chem, 2010. **391**(12): p. 1441-9.
38. Graupera, I., et al., *Adipocyte Fatty-Acid Binding Protein is Overexpressed in Cirrhosis and Correlates with Clinical Outcomes*. Sci Rep, 2017. **7**(1): p. 1829.
39. Masetti, M., et al., *Adipocyte-fatty acid binding protein and non-alcoholic fatty liver disease in the elderly*. Aging Clin Exp Res, 2014. **26**(3): p. 241-7.
40. Jeppesen, J., et al., *FAT/CD36 is localized in sarcolemma and in vesicle-like structures in subsarcolemma regions but not in mitochondria*. J Lipid Res, 2010. **51**(6): p. 1504-12.

41. Schaefer, C.F., et al., *PID: the Pathway Interaction Database*. Nucleic Acids Res, 2009. **37**(Database issue): p. D674-9.
42. van den Beukel, J.C., et al., *Cold Exposure Partially Corrects Disturbances in Lipid Metabolism in a Male Mouse Model of Glucocorticoid Excess*. Endocrinology, 2015. **156**(11): p. 4115-28.
43. Spiga, F., et al., *HPA axis-rhythms*. Compr Physiol, 2014. **4**(3): p. 1273-98.
44. van den Heuvel, J.K., et al., *Identification of a selective glucocorticoid receptor modulator that prevents both diet-induced obesity and inflammation*. Br J Pharmacol, 2016. **173**(11): p. 1793-804.
45. Mammi, C., et al., *A novel combined glucocorticoid-mineralocorticoid receptor selective modulator markedly prevents weight gain and fat mass expansion in mice fed a high-fat diet*. Int J Obes (Lond), 2016. **40**(6): p. 964-72.
46. Lonardo, A., et al., *Review article: hepatic steatosis and insulin resistance*. Aliment Pharmacol Ther, 2005. **22 Suppl 2**: p. 64-70.
47. De Bosscher, K., et al., *Selective transrepression versus transactivation mechanisms by glucocorticoid receptor modulators in stress and immune systems*. Eur J Pharmacol, 2008. **583**(2-3): p. 290-302.
48. Imprialos, K.P., et al., *The potential role of statins in treating liver disease*. Expert Rev Gastroenterol Hepatol, 2018. **12**(4): p. 331-339.
49. Seif El-Din, S.H., et al., *Effects of rosuvastatin and/or beta-carotene on non-alcoholic fatty liver in rats*. Res Pharm Sci, 2015. **10**(4): p. 275-87.
50. Sundahl, N., et al., *Selective glucocorticoid receptor modulation: New directions with non-steroidal scaffolds*. Pharmacol Ther, 2015. **152**: p. 28-41.

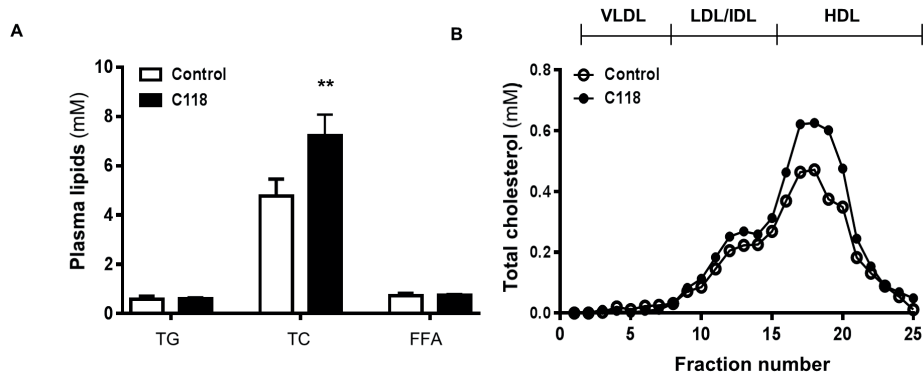
## APPENDIX

Supplementary Table 1- Primer sequences that were used for RT- qPCR analysis

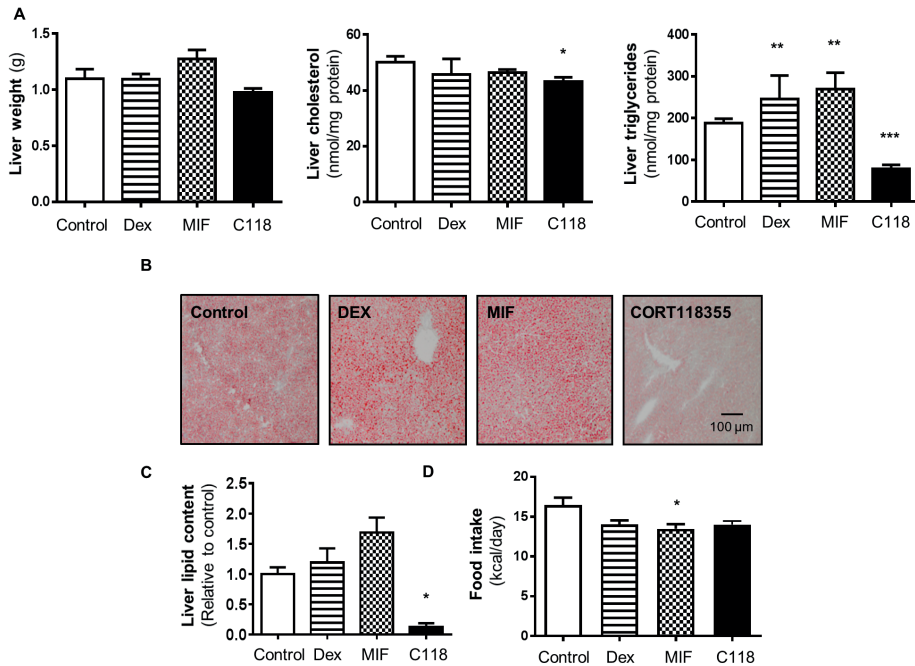
Gene	Forward primer sequence	Reverse primer sequence
<i>Acc1</i>	AACGTGCAATCCGATTTGTT	GAGCAGTTCTGGGAGTTTCG
<i>Acc2</i>	AGATGGCCGATCAGTACGTC	GGGGACCTAGGAAAGCAATC
<i>ApoB</i>	GCCCATTTGTGGACAAGTTGATC	CCAGGACTTGAGAGTCTTGGGA
<i>Cd36</i>	GCAAAGAACAGCAGCAAAATC	CAGTGAAGGCTCAAAGATGG
<i>Cpt1</i>	GAGACTTCCAACGCATGACA	ATGGGTTGGGGTGATGTAGA
<i>Dgat2</i>	TCGCGAGTACCTGATGTCTG	CTTCAGGGTGACTGCGTTCT
<i>Fabp1</i>	GAGGAGTGCGAAGTGGAGAC	GTAGACAATGTCGCCAATG
<i>Fasn</i>	GCGCTCCTCGCTTGTCTCT	TAGAGCCCAGCCTTCCATCTCCTG
<i>G6p</i>	TCCTCTTCCCATCTGGTTC	TATACACCTGCTGCGCCCAT
<i>Mttp</i>	CTCTTGGCAGTGCTTTTTCTCT	GAGCTTGATAGCCGCTCATT
<i>Pepck</i>	ATCTTTGGTGGCCGTAGACCT	GCCAGTGGGCCAGGTATTT
<i>Srebp1c</i>	AGCCGTGGTGAGAAGCGCAC	ACACCAGGTCCTTCAGTGATTTGCT



**Supplementary Figure 1: CORT118335 prevents lipid accumulation and inflammation in liver and white adipose tissue.** In a preventive setting, mice received 10% fructose water with high-fat diet containing vehicle or CORT118335 (C118) for three weeks (n=8 per group). CORT118335 reduced A) gonadal white adipocyte size (H&E staining), B) gonadal white adipose tissue weight, C) F4/80 immunostaining in gWAT, D) liver lipids stained with oil red O, E) liver weight and F) hepatic F4/80 immunostaining. \* =  $p < 0.05$ , \*\*\* =  $p < 0.001$  vs control.

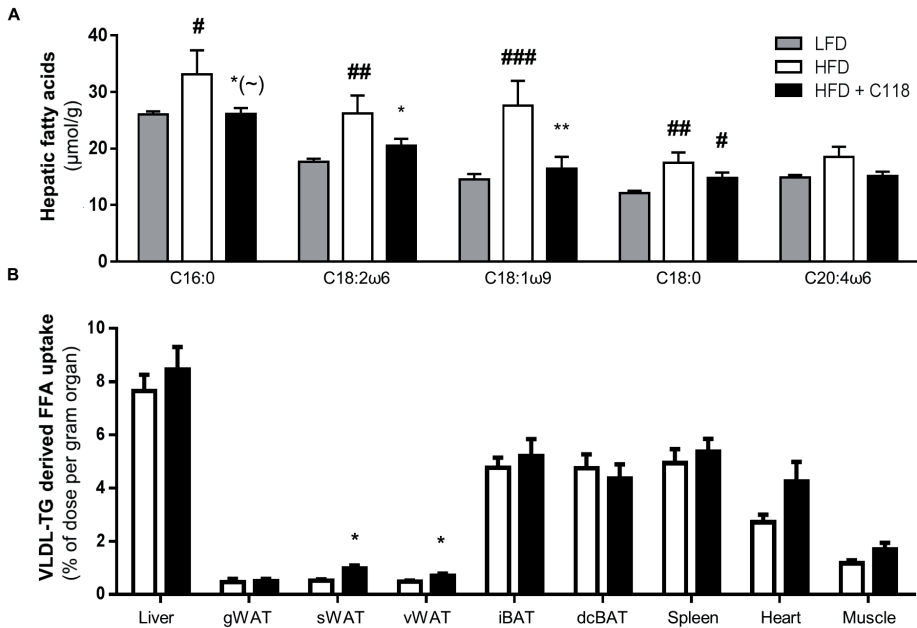


Supplementary Figure 2: CORT118335 elevates plasma cholesterol levels. In a preventive setting, mice received 10% fructose water with high-fat diet (HFD) containing vehicle or CORT118335 (C118) for three weeks (n=8 per group). Effects of C118 on A) plasma lipids and B) lipoprotein profile after two weeks of C118 treatment. \*\* =  $p < 0.01$  vs control.

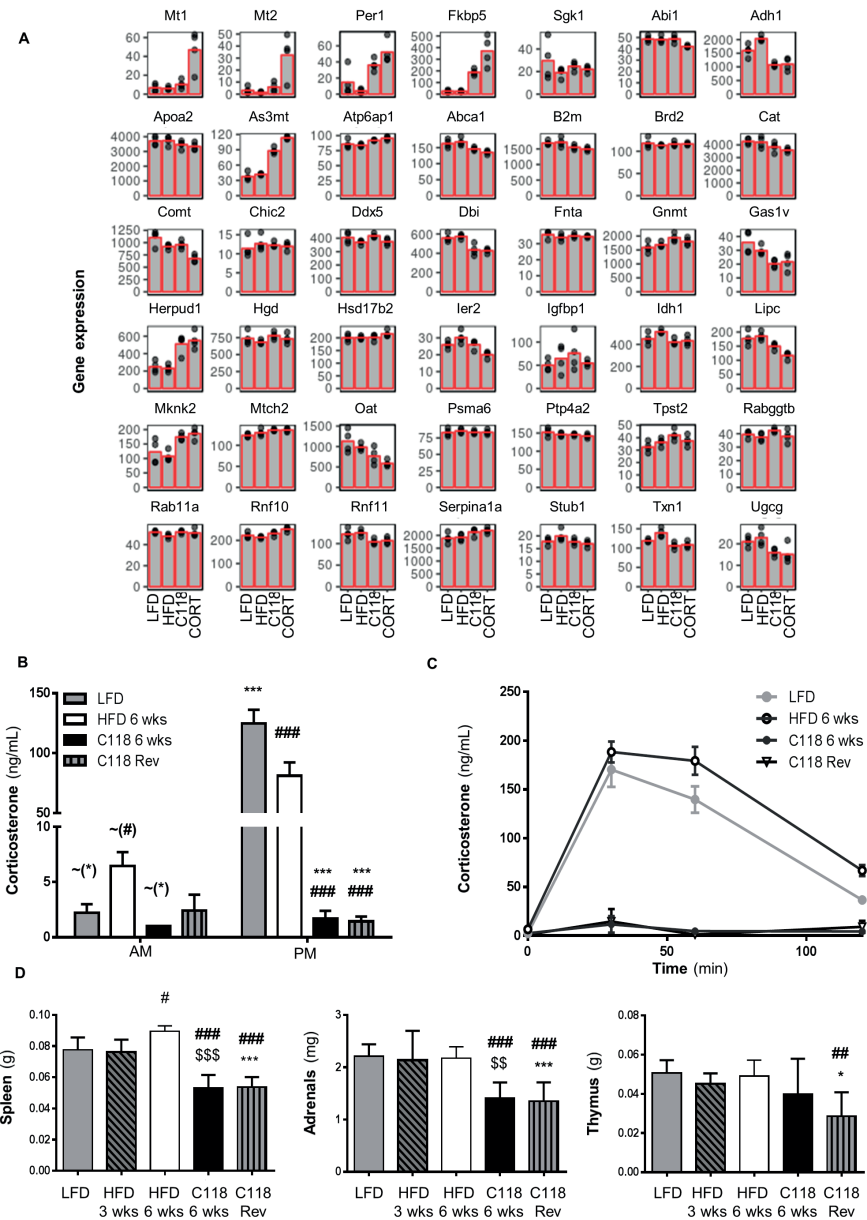


Supplementary Figure 3: Dexamethasone and mifepristone do not positively affect hepatic lipid accumulation. In a preventive setting, mice received high-fat diet containing vehicle, dexamethasone (Dex) or mifepristone (MIF) for three weeks (n=8 per group). A) Dex and MIF increased liver weight, hepatic triglycerides and cholesterol and B-C) hepatic lipids stained with oil red O. D) Only MIF reduced food intake in week 1. \* =  $p < 0.05$ , \*\* =  $p < 0.01$ , \*\*\* =  $p < 0.001$ .



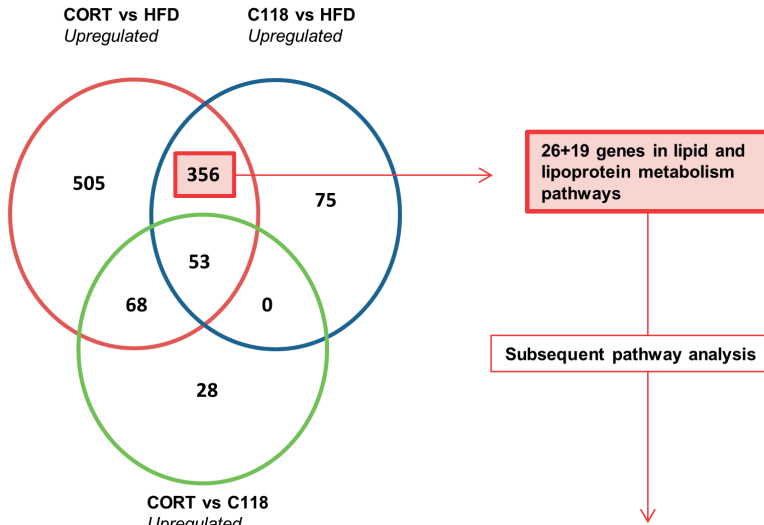


**Supplementary Figure 4: CORT118335 does not alter hepatic uptake of VLDL-derived fatty acids.** In a preventive setting, mice received 10% fructose water with high-fat diet (HFD) containing vehicle or CORT118335 (C118) for three weeks (n=8 per group). A) C118 reduced virtually all types of LCFA in the liver in week 3. B) Mice received low-fat diet (LFD), HFD supplemented with vehicle or C118 for six weeks (n=8 per group). C118 did not alter VLDL-derived fatty acid uptake measured as uptake from radioactive labelled triglycerides packaged in VLDL-like particles in week 3. \*(-) =  $p < 0.01$ , \* =  $p < 0.05$ , \*\* =  $p < 0.01$  vs HFD control; # =  $p < 0.05$ , ## =  $p < 0.01$ , ### =  $p < 0.001$  vs LFD.



Supplementary Figure 5: CORT118335 mostly acts as partial agonist on *in vivo* HPA-axis activity markers. A) Expression of GR target genes in livers of mice that received low-fat diet (LFD), high-fat diet (HFD) supplemented with vehicle, CORT118335 (C118) or corticosterone for two days ( $n=4$  per group). B-D) In a reversal setting, mice received a LFD, 10% fructose water and a HFD supplemented with vehicle or C118 for six weeks (Reversal). At the beginning of week 6, corticosterone levels were measured in plasma collected at 18:00 (PM). The next day at 8:00 (AM) and during the subsequent novelty stress test, plasma was collected for corticosterone and ACTH measurements. D) C118 reduced tissue weights of spleen, adrenals and thymus.  $-(*), * = p < 0.05, ** = p < 0.01, *** = p < 0.001$  vs HFD 3 wks;  $-(\#), \# = p < 0.05, \#\# = p < 0.01, \#\#\# = p < 0.001$  vs LFD;  $\$\$ = p < 0.01, \$\$\$ = p < 0.001$  vs HFD 6 wks.

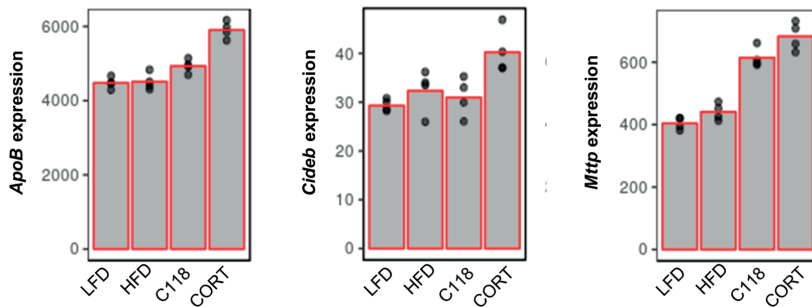
A



B

Pathway name	Number of genes	P-value
Metabolism of lipids and lipoproteins	26	8,17E-32
Lipid metabolism	19	1,03E-23
Phospholipid metabolism	11	1,52E-14
Fatty acid, triacylglycerol, and ketone body metabolism	9	4,06E-11
Glycerophospholipid biosynthetic process	6	1,53E-08
Ppara activates gene expression	6	5,62E-08
Regulation of cholesterol biosynthesis by srebp (srebf)	5	6,60E-08
Regulation of lipid metabolism by peroxisome proliferator-activated receptor alpha (pparalpha)	6	6,61E-08
Protein biosynthesis	11	1,75E-07
Thiele2013 - human metabolism global reconstruction (recon 2)	13	3,17E-07
Cholesterol metabolic process	5	4,10E-07
Fatty acid metabolism pathway	5	2,21E-06
Synthesis of pe	3	2,38E-06
PI metabolism	4	3,45E-06
Triglyceride biosynthetic process	4	5,27E-06
Fatty acid oxidation	4	6,00E-06
Synthesis of pc	3	8,60E-06
3-phosphoinositide biosynthesis	3	2,58E-05
Synthesis of pips at the plasma membrane	3	4,49E-05

C



← **Supplementary Figure 6: Both CORT118335 and corticosterone treatment upregulate expression of genes within *de novo* lipogenesis and beta-oxidation pathways.** RNA sequence analysis was performed on livers of mice that received a low-fat diet (LFD), 10% fructose water and a high-fat diet (HFD) supplemented with vehicle, CORT118335 (C118) or corticosterone (CORT) for two days (n=4 per group). A) Venn diagram of overlap in upregulated genes between differential regulated genes in comparisons 1) CORT vs HFD, 2) C118 vs HFD and 3) CORT vs C118. B) 45 genes within lipid and lipoprotein pathways were found after pathway analysis on 356 genes regulated by both GR ligands to a similar expression level. Subsequent pathway analysis on these 45 genes identified the pathways 'Triglyceride biosynthetic pathway' and 'Fatty acid oxidation' (red box). C) Expression of genes within the VLDL pathway.

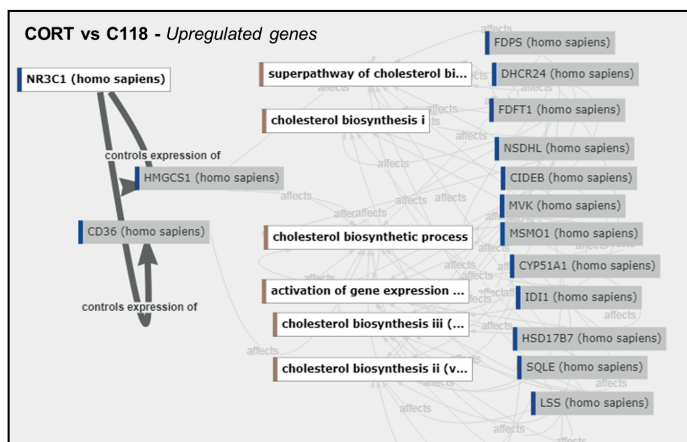
A

Pathway name	Number of	P-value
Thiele2013 - human metabolism global reconstruction (recon 2)	57	1,85E-10
Glycolysis pathway	7	2,47E-06
Gluconeogenesis	11	2,76E-06
Glucose metabolism	17	2,77E-06
Il6-mediated signaling events	8	3,89E-06
Carbohydrate metabolism	18	4,02E-06
Metabolism of lipids and lipoproteins	26	6,87E-06
Lipid metabolism	19	1,41E-05
Glycolytic process through glucose-6-phosphate	6	2,57E-05
P38 mapk signaling pathway pid	7	3,34E-05

B

Pathway name	Number of genes	P-value
cholesterol biosynthetic process	14	2,66E-18
metabolism of lipids and lipoproteins	30	2,42E-17
superpathway of cholesterol biosynthesis	11	3,56E-16
cholesterol biosynthesis ii (via 24,25-dihydrolanosterol)	7	3,62E-11
cholesterol biosynthesis iii (via desmosterol)	7	3,62E-11
cholesterol biosynthesis i	7	3,62E-11
sterol biosynthesis pathway	7	2,69E-10
phase 1 - functionalization of compounds	10	1,05E-09
activation of gene expression by srebf (srebp)	8	1,47E-09
biological oxidations	12	1,01E-08

C



D

Pathway name	Number of genes	P-value
cytokine signaling in immune system	14	3,07E-08
interferon signaling	10	7,08E-07
drug metabolism by cytochrome p450 pathway	5	3,05E-06
jak-stat signaling pathway	6	4,35E-06
metabolism of xenobiotics by cytochrome p450 pathway	5	5,66E-06
biological oxidations	9	5,99057E-06
retinol metabolism pathway	5	1,10643E-05
linoleic acid metabolism pathway	4	1,57707E-05
drug metabolism	5	1,77388E-05
type ii interferon signaling pathway	6	1,91502E-05

← **Supplementary Figure 7: Both CORT118335 and corticosterone regulate expression of genes enriched in glucose and lipid metabolism pathways.** RNA sequence analysis was performed on livers of mice that received a low-fat diet (LFD), 10% fructose water and a high-fat diet (HFD) supplemented with vehicle, CORT118335 or corticosterone for two days (n=4 per group). Results of pathway analysis on A) 356 genes regulated by both GR ligands *to a similar expression level* and B) all *upregulated* genes within the corticosterone vs CORT118335 comparison. C) In the latter comparison, relationships between all genes within cholesterol pathways and '*Nr3c1*' (glucocorticoid receptor gene) were investigated. D) Results of pathway analysis of all *downregulated* genes within the corticosterone vs CORT118335 comparison.

